

Fracture toughness and tensile properties of nano-structured ferritic steel 12YWT

M.A. Sokolov *, D.T. Hoelzer, R.E. Stoller, D.A. McClintock

Oak Ridge National Laboratory, Oak Ridge, TN 37831-6151, USA

Abstract

The oxide dispersion strengthened (ODS) steels are being developed and investigated for fission and fusion structural applications in Japan, Europe, and the United States. In this paper, the fracture toughness and tensile properties of an ODS steel with nominal composition Fe–12Cr–2.5W–0.4Ti–0.25Y₂O₃ (designated 12YWT) were investigated and compared to commercial reduced-activation ferritic/martensitic (RAFM) steels. Small, 1.6-mm thick and 3.2-mm wide, 3-point bend specimens were used for fracture toughness characterization of this steel. Specimens were fatigue pre-cracked to initial crack length (a) to width (W) ratio of 0.45 and tested quasi-statically in the temperature range from -50 °C to 550 °C. Specimens tested up to 50 °C exhibited elastic–plastic cleavage fracture that was typical for the transition region in ferritic steels. The master curve transition temperature, T_0 , for the 12YWT alloy was determined to be 102 °C. Specimens tested at 100 °C and higher exhibited ductile stable crack growth. In these cases, the J -integral at the onset of stable crack growth (J_{Ic}) was determined from the J – R curves. Their equivalent values in terms of stress intensity factor, K_{Jic} , were about 93 MPa \sqrt{m} at 100 °C and decreased to 53 MPa \sqrt{m} at 550 °C. This study showed that oxide dispersion strengthening resulted in significant decreases in the toughness properties compared to commercial RAFM steels, although appreciable level of toughness was still retained. Tensile tests were performed at temperatures between room temperature and 800 °C. As expected, this material exhibited very high yield strength, ~ 1300 MPa, at room temperature. For comparison, the yield strength of commercial RAFM steels is about 550 MPa. Yield strength of 12YWT decreases as test temperature increases and at 800 °C it is about 323 MPa.

© 2007 Elsevier B.V. All rights reserved.

1. Introduction

The reduced-activation ferritic/martensitic (RAFM) steels are the primary candidates for a fusion power plant first wall and blanket structures. Ferritic–martensitic steels are known to resist radiation swelling and have good thermal conductivity. However, their

utilization is limited to around 600 °C due to insufficient tensile and creep strengths at higher temperatures. One way to increase the temperature capabilities of RAFM steels is by incorporation of an oxide dispersion. Oxide dispersion strengthening (ODS) of ferritic steels is a well known process to improve their strength and creep properties. However, recent advances in manufacturing and understanding of the strengthening mechanisms resulted in creation of a new type of material, referred to as nano-structured ferritic (NSF) steels. In the case

* Corresponding author. Tel.: +1 865 574 4842; fax: +1 865 574 0641.

E-mail address: sokolovm@ornl.gov (M.A. Sokolov).

of NSF steels, oxide particles in the nanometer size range are produced, resulting in significant improvement in strength and creep properties of steels even compared to the conventional ODS steels without nano-size oxide particles. Elevated temperature strength in these steels is obtained by a high number density of ultrafine, nanometer-scale yttria–titanium–oxygen complex particles dispersed in a ferritic matrix. These particles have been shown to be clusters of atoms, similar to Guinier–Preston zones in the Al–Cu system [1].

The NSF steel investigated in this study was prepared by mechanically alloying (MA) of a pre-alloyed Fe–12.3%Cr–3%W–0.39%Ti (wt%) powder with 20-nm size 0.25 wt% Y₂O₃ powder [1,2]. The milled powders were canned in mild steel and consolidated into bar by hot extrusion at 1150 °C, followed by a series of rolling operations at elevated temperatures and annealings at 1050 °C for 1 h. The ultrafine-scale microstructure of the 12YWT NSF ferritic alloy has been characterized by atom probe tomography in the as-received condition, after extended high temperature creep tests, and after high temperature isothermal heat treatments at temperatures up to 1300 °C (~85% of melting temperature) [3]. Atom probe tomography revealed the presence of a high number density, $1.4 \times 10^{24} \text{ m}^{-3}$, of 2–4 nm diameter yttrium-, titanium-, and oxygen-enriched clusters in the as-received 12YWT alloy. The Ti and O levels in the particles were higher than the Y level. Furthermore, the average size of the particles produced by mechanical alloying was significantly smaller than the initial size of the Y₂O₃ particles. Atom probe tomography also revealed that these ultrafine particles were extremely resistant to coarsening during creep and isothermal aging at 1300 °C. Solute segregation of the alloying elements to the dislocations and grain boundaries was also observed. The ultrafine particles and the solute segregation to the dislocations will inhibit dislocation movement, and their stability may explain the improved high temperature mechanical properties.

2. Tensile properties

Tensile tests were performed at temperatures between room temperature and 800 °C. This material exhibited a very high yield strength, ~1300 MPa, and ultimate strength, ~1400 MPa, in the longitudinal direction at room temperature. The yield strength decreases as test temperature

increases, but remains higher than conventional RAFM steels, Fig. 1. For comparison, the yield strength of conventional 9Cr–2WVTa RAFM steel is about 550 MPa at room temperature [4]. The present results show that the 12YWT alloy is stronger in the transverse than in the longitudinal direction up to 500 °C. Between 500 and 650 °C, strength in both directions becomes more similar. Finally, this alloy becomes stronger in the longitudinal direction above ~650 °C, see Fig. 2. The uniform elongation of transverse specimens increases with of temperature, while longitudinal specimens exhibited the opposite temperature dependence, see Fig. 3.

All of the above tests were performed with a strain rate of $1 \times 10^{-3} \text{ s}^{-1}$. To study the strain rate

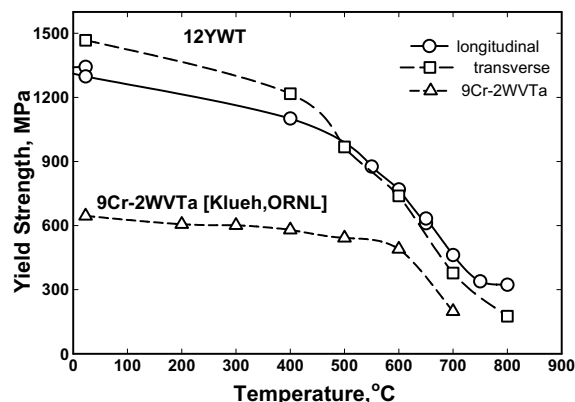


Fig. 1. Temperature dependence of yield strength of nanostructured alloy 12YWT compared to conventional ferritic-martensitic steel 9Cr–2WVTa.

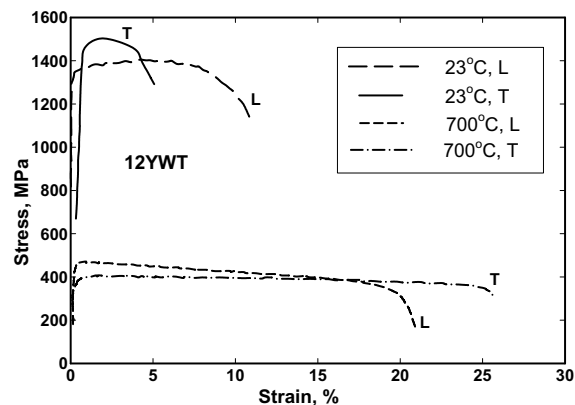


Fig. 2. Stress–strain curves of 12YWT alloy in longitudinal (L) and transverse (T) directions at room temperature and 700 °C.

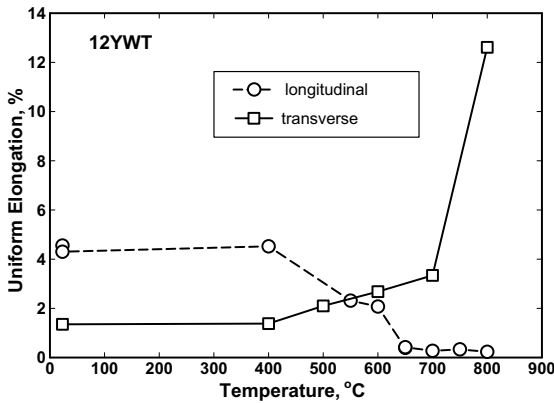


Fig. 3. Temperature dependence of uniform elongation of nano-structured alloy 12YWT in longitudinal and transverse directions.

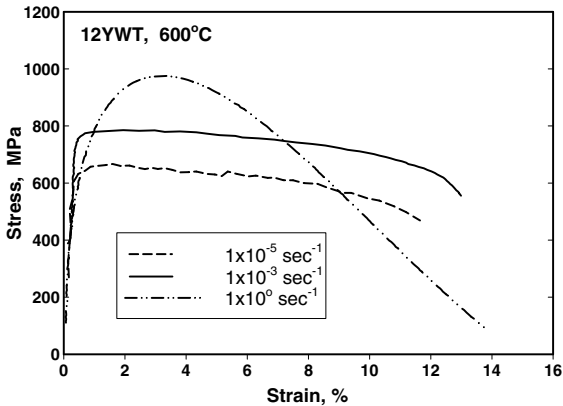


Fig. 4. Stress–strain curves of 12YWT alloy at 600 °C at strain rates of 1×10^{-5} , 1×10^{-3} , and $1 \times 10^0 \text{ s}^{-1}$.

effect on tensile data, additional tests of longitudinal specimens were performed with strain rates of $1 \times 10^{-5} \text{ s}^{-1}$ and $1 \times 10^0 \text{ s}^{-1}$ at 600 °C, see Fig. 4. This alloy exhibited a strong strain rate dependence, with ultimate strength and total elongation increasing as strain rate increases from $1 \times 10^{-5} \text{ s}^{-1}$ to $1 \times 10^0 \text{ s}^{-1}$. The overall shape of the tensile traces at $1 \times 10^{-5} \text{ s}^{-1}$ and $1 \times 10^{-3} \text{ s}^{-1}$ appears to be similar, but the shape of the tensile trace changes considerably at $1 \times 10^0 \text{ s}^{-1}$, see Fig. 4.

3. Fracture toughness properties

Fracture toughness characterization of the 12YWT alloy was performed by slow 3-point bend testing in general accordance with the ASTM E1921-02 standard. Specimens of 3.3 mm width

(*W*) and 1.7 mm thickness (*B*) were machined in the L–T orientation and tested with a span (*S*) of 13.3 mm ($S/W = 4$). This orientation was selected because of the anisotropic microstructure that was observed by transmission electron microscopy in the 12YWT alloy, which consisted of elongated grains that were $\sim 1 \mu\text{m}$ thick and $\sim 5\text{--}20 \mu\text{m}$ in length. The specimens were fatigue pre-cracked before testing to a ratio of crack length to specimen width of about 0.45. Tests were conducted in the temperature range from $-50 \text{ }^\circ\text{C}$ to $550 \text{ }^\circ\text{C}$. The temperatures were maintained within $\pm 2 \text{ }^\circ\text{C}$ during the tests.

Six specimens were tested in the range from $-50 \text{ }^\circ\text{C}$ to $50 \text{ }^\circ\text{C}$, which all failed by brittle instability. Fracture toughness, K_{Jc} , varied from 41 to $84 \text{ MPa}\sqrt{\text{m}}$. The master curve concept was used to characterize ductile-to-brittle transition fracture toughness of 12YWT alloy by means of reference transition temperature, T_0 . Because of the high strength, all of K_{Jc} data satisfy validity requirements of ASTM E1921-02 standard despite small specimen size. The reference fracture toughness transition temperature, T_0 , for the 12YWT alloy was determined to be $102 \text{ }^\circ\text{C}$. This is a high absolute value of T_0 compared to a T_0 value of about $-100 \text{ }^\circ\text{C}$ for conventional RAFM steels like F82H [5], see Fig. 5.

In the fully ductile region, the values of stress intensity factor converted from the critical *J*-integral at the onset of stable crack growth, K_{Jc} , were about $93 \text{ MPa}\sqrt{\text{m}}$ at $100 \text{ }^\circ\text{C}$ and decreased to $80 \text{ MPa}\sqrt{\text{m}}$ at $450 \text{ }^\circ\text{C}$ and to $53 \text{ MPa}\sqrt{\text{m}}$ at $550 \text{ }^\circ\text{C}$. While those are relatively high toughness values, nevertheless, they are significantly lower than K_{Jc} values for the

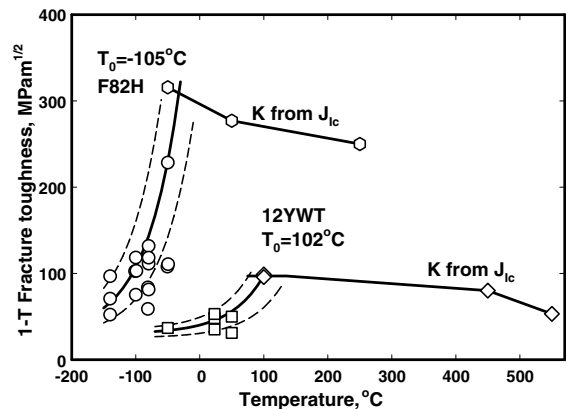


Fig. 5. Fracture toughness of 12YWT alloy compared to conventional RAFM steel, F82H.

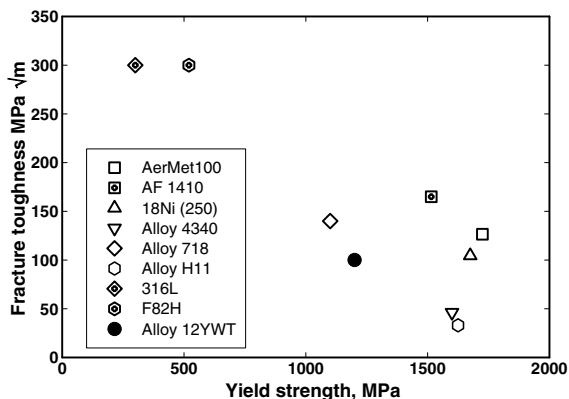


Fig. 6. Comparison of the upper-shelf fracture toughness value of 12YWT alloy with fracture toughness of different high-strength alloys, conventional RAFM steel, F82H, and stainless steel, 316L.

conventional RAFM steel F82H. On the other hand, these upper shelf fracture toughness data are in general agreement with fracture toughness data for some other high-strength alloys, see Fig. 6.

This study showed that addition of a nanometer-scale oxide dispersion resulted in significant decreases in the toughness properties compared to commercial RAFM steels, although an appreciable level of toughness was still retained. Further work with thermo-mechanical treatment of this alloy needs to be done to optimize the strength-toughness relationship.

4. Summary

1. 12YWT alloy exhibited high yield (~ 1300 MPa) and ultimate (~ 1400 MPa) strengths at room temperature. Yield and ultimate strengths decrease as test temperature increases, but remain higher than for conventional RAFM steels.
2. Strength of 12YWT alloy exhibited a slight orientation dependence that changes with increasing temperature, while a more significant effect was observed on uniform elongation.
3. The uniform elongation of transverse specimens increases with temperature and longitudinal specimens exhibited the opposite temperature dependence.
4. This alloy exhibited a strong strain rate dependence. Strength and total elongation increase as

strain rate increases from $1 \times 10^{-5} \text{ s}^{-1}$ to $1 \times 10^0 \text{ s}^{-1}$.

5. The reference fracture toughness transition temperature, T_0 , was determined to be 102°C . This is a high absolute value of T_0 compared to $\sim -100^\circ\text{C}$ for conventional RAFM steels like F82H.
6. In the fully ductile region, the values of stress intensity factor converted from the critical J -integral at the onset of the stable crack growth, $K_{J_{IC}}$, were about $93 \text{ MPa}\sqrt{\text{m}}$ at 100°C and decreased to $80 \text{ MPa}\sqrt{\text{m}}$ at 450°C and to $53 \text{ MPa}\sqrt{\text{m}}$ at 550°C . These upper shelf fracture toughness data are in general agreement with fracture toughness data for some other high-strength alloys.

Overall, this study showed that oxide dispersion of 12YWT alloy resulted in a significant increase in the strength properties and decrease in the toughness properties compared to commercial RAFM steels. However, an appreciable level of toughness was still retained.

Acknowledgements

This research was sponsored by the Office of Nuclear Energy, Science and Technology (I-NERI 2001-007-F), US Department of Energy (DOE) and the Laboratory Directed Research and Development Program of Oak Ridge National Laboratory, managed by UT-Battelle, LLC for the US DOE under Contract No. DE-AC05-00OR22725.

The authors would like to thank T.S. Byun from Oak Ridge National Laboratory for his assistance with high temperature fracture toughness tests.

References

- [1] D.J. Larson, P.J. Maziasz, I.-S. Kim, K. Miyahara, *Scr. Mater.* 44 (2001) 359.
- [2] I.-S. Kim, J.D. Hunn, N. Hashimoto, D.J. Larson, P.J. Maziasz, R.L. Klueh, K. Miyahara, E.H. Lee, *J. Nucl. Mater.* 280 (2000) 264.
- [3] M.K. Miller, E.A. Kenik, K.F. Russell, L. Heatherly, D.T. Hoelzer, P.J. Maziasz, *Mater. Sci. Eng. A353* (2003) 140.
- [4] R.L. Klueh, *Metall. Trans.* 20A (1989) 463.
- [5] M.A. Sokolov, R.L. Klueh, G.R. Odette, K. Shiba, H. Tanigawa, *ASTM STP 1447*, 2003.